Study of Characteristic of Flow Passed Actuator Arm by Large Eddy Simulation Method

Presented in 1st Data Storage Technology Conference (DST-CON 2008)

Jarupol Suriyawanakul and Kiatfa Tangchaichit*

Abstract

This paper contains and investigates the air flow characteristics which affect the actuator arm at the varied positions. Simulation models have been built by the simple model which considers only area around the arm. The velocity profile is referred to 3.5″ hard disk drive and the speed of media is 7,200 rpm. Regarding to Large Eddy Simulation method, the result shows that the position that suffers the most effects from the flow is the inner diameter position. The result can be seen in the power spectral density graph and flow characteristics.

Keywords: Air flow, actuator arm, hard disk drive, large eddy simulation method

Introduction

According to the continuous development of hard disk drive makes the Arial Density of data recording higher. It means that the processing of the inner part of the hard disk must be more accurate. Therefore, a little of vibration can effect to the read/write head operation. So the study of hard disk aerodynamic has become more important. Due to a high rotation speed of media, the actuator arm is affected by its operation which always against the flow. And this condition can be the source of vibration of itself. This paper will describe the flow characteristic when it passes through the arm.

The effect of actuator arm shape has been studied by Ong et al. (2000) they studied a systematic way of estimating the optimal arm length of an actuator arm to get higher bandwidth. They found the actuator with triangular edge gave lower TMR. Kubotera et al.(2002) and Tsuda et al.(2003) they studied flow structure in 3.5″ hard disk drive with rotation speed 10,033 rpm by difference kinds of actuator arm. First is actuator arm with weight saving hole and the other is without weight saving hole. With Direct Numerical Simulation (DNS) method they found the vortex at downstream of the hole case was larger than the without hole case. And these flows can be considered to be the excitation source which affect to the actuator arm. Kaneko et al. (2007) have developed the experiment to simulate the flow across the actuator arm in water tunnel by enlarged the model ten times larger which base on Reynolds number similarity. They found the dynamic lift with the spectral peak was induced from the vortex shedding from the trailing edge of the arm. And the

Department of Mechanical Engineering, Faculty of Engineering, Khon Kaen University, Maung, Khon Kaen 40000 Thailand
**corresponding author; e-mail: 4950400110@kku.ac.th.*

วารสารวิจัย มข. 13 (3) : เมษายน 2551

dynamic lift can be reduced by modification of trailing edge shape of the arm. Shimizu et al. studied an aerodynamic characteristics in hard disk drive by Large Eddy Simulation (LES) method. They found two types of the pressure fluctuation. One is between the facing of suspension that is vibration source of the suspensions. The other is the downstream flow fluctuation of the arm that may cause disk vibration.

We used an unsteady LES to study flow characteristics when air flow passed the arm at each position. For reducing time consumption we had to simplify our model to consider only area around actuator arm which extended to the media.

Computational methods

We use the commercial software Fluent and Gambit for creating and calculating our model.

The governing equations are the Navier-Stokes equation

$$\frac{\partial \rho u_i}{\partial t} + \frac{\partial \rho u_i u_j}{\partial x_j} = -\frac{\partial \bar{p}}{\partial x_i} + \frac{\partial}{\partial x_j}\left(\mu\left(\frac{\partial u_i}{\partial x_j} + \frac{\partial u_j}{\partial x_i}\right)\right) \qquad (1)$$

and equation of continuity

$$\frac{\partial u_i}{\partial x_i} = 0 \qquad (2)$$

and the Large-Eddy Simulation model was used for calculating turbulent flows by filtering the N-S equation (1) and (2) as

$$\frac{\partial \rho \bar{u}_i}{\partial t} + \frac{\partial \rho \bar{u}_i \bar{u}_j}{\partial x_j} = -\frac{\partial \bar{p}}{\partial x_i} + \frac{\partial}{\partial x_j}\left(\mu\left(\frac{\partial \bar{u}_i}{\partial x_j} + \frac{\partial \bar{u}_j}{\partial x_i}\right) - \tau_{ij}\right) \qquad (3)$$

and

$$\frac{\partial \bar{u}_i}{\partial x_i} = 0 \qquad (4)$$

where

$$\tau_{ij} = -\rho\left(\overline{u_i u_j} - \bar{u}_i \bar{u}_j\right) \qquad (5)$$

and $\bar{u}_i$ is the filtered instantaneous velocity.

A second-order upwind scheme was used to discretize the momentum equation and a second order was used to discretize the pressure. And SIMPLEC algorithm has used for Pressure-Velocity Coupling.

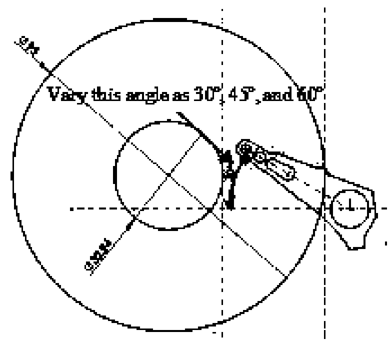

Figure 1. Outline of original model.

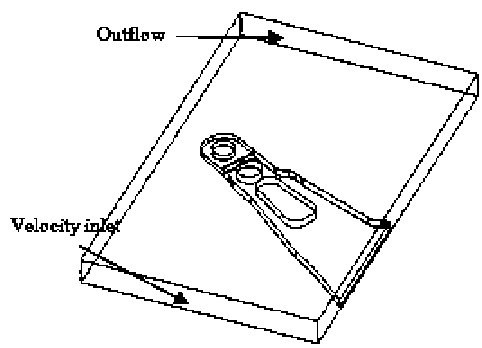

Figure 2. Computational model.

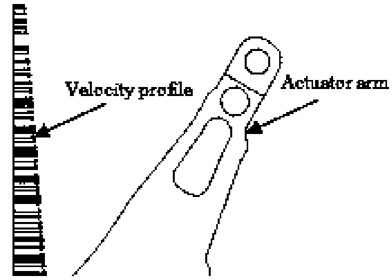

Figure 3. Outline of original model.

This study uses the Smagorinsky-Lilly model to model the Subgrid-Scale model. By LES method will reduce time consumption from DNS method and get higher precision than RANS method.

Computational models

We simplified the model from Figure 1. to Figure 2. to reduce complexity of original model.

From Figure 3, we have defined a velocity inlet profiles by refer to angular velocity of disc which rotate at 7,200 rpm as

$$v = \omega r \qquad (6)$$

where $16.47mm. \leq r \leq 47.5mm.$ and

Table 1. Computational conditions

Quantity	Condition
Arm Mesh Size(mm)	0.2
Other Volume Mesh Size(mm)	0.4
Element	Tet/Hybrid
Mesh Type	Tgrid
Number of Mesh	400,242
Solver	Segregate
Formulation	Implicit
Time	Unsteady
Unsteady Formulatiom	2nd-Order Implicit
Model	Large Eddy Simulation
Subgrid-Scale Model	Smagorinsky-Lilly
Pressure-Velocity Coupling	SIMPLEC
Pressure Discretization	second order
Momentum Discretization	second order upwind
Discretization Flow	Low Diffusion Second Order
Convergence Criterian	1.00E-06
Time Step Size(s)	1.00E-06
Total Number of Time Steps	15,000 (15ms)

$$\omega = 2\pi \left(\frac{7200}{60}\right) \qquad (7)$$

Our computational conditions have shown in Table 1. And we consider the range of time step between 4,000 to 15,000 time steps that the flow has become fully develop. All of wall conditions except velocity inlet and outflow are defined as wall with no-slip condition. The position of the arm was varied at 3 different positions which are 30°, 45° and 60° as shown in Figure 1.

Result

A. Path lines

Figure 4, 5 and 6 are the path lines of velocity which release from the front arm at position 30°, 45° and 60° respectively.

We found that they have same flow direction when they flow pass the arm. First flow move to the weight saving hole in A direction and drop to the hole in B direction then split out from the hole and mixed with the flow which flow across the arm and flow out to downstream at C direction. Because of these characteristics the flow at downstream has diffused as shown in zone D. And this mixed flow could be the source of arm vibration and disc flutter.

B. Contours

According to the spreading flow at zone D of path lines figures, From Figure 7, 8 and 9 the contour of velocity in surface view by comparing with 3 layers show flooding of the turbulent flow at zone E is wider than the other zone. This effect is from the mixing flow between flow from weight saving hole and flow across the arm.

C. Mean Static Pressure

From Figure 10 we show the mean static pressure at each position. The chart show at 30° has higher pressure than other positions. And on back arm has higher pressure than other surface.

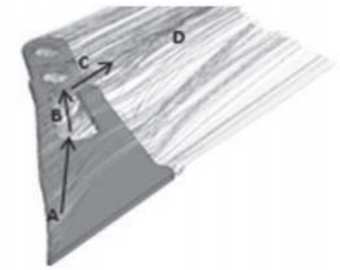

Figure 4. Velocity Magnitude Path Lines at 30°.

Figure 5. Velocity Magnitude Path Lines at 45°.

Figure 6. Velocity Magnitude Path Lines at 60°

D. Power Spectrum Density

According to the pressure which is the most effect to track mis-registration of the arm are on front arm and back arm. By Fast Fourier Transform (FFT) analysis of the static pressure on back arm and front arm surface as shown in Figure 11 and 12 at range near 5e-10^{-3}Hz, we found the PSD of back arm and front arm at 30° position is the highest and 45° is the second and 60° is the last. It means at the 30° has the most effect from wind disturbance. The PSD of back arm is higher than front arm this may cause of drag force at downstream of the arm.

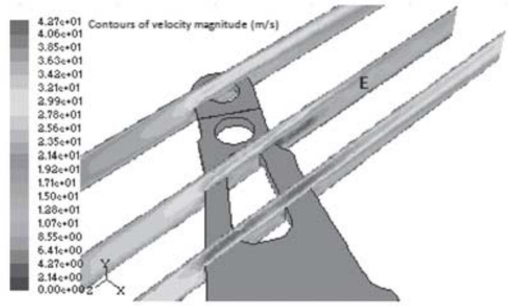

Figure 7. Velocity Magnitude Contour (m/s) at 30°.

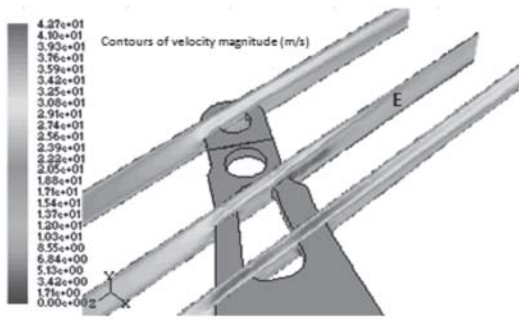

Figure 8. Velocity Magnitude Contour (m/s) at 45°.

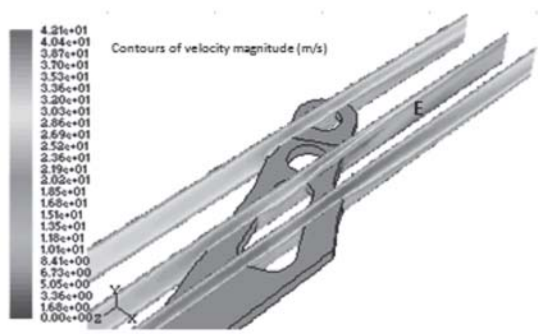

Figure 9. Velocity Magnitude Contour (m/s) at 60°.

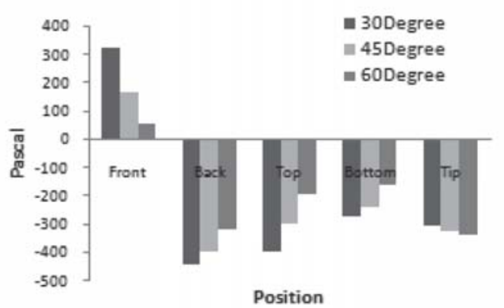

Figure 10. Mean Static Pressure at each surface on the arm.

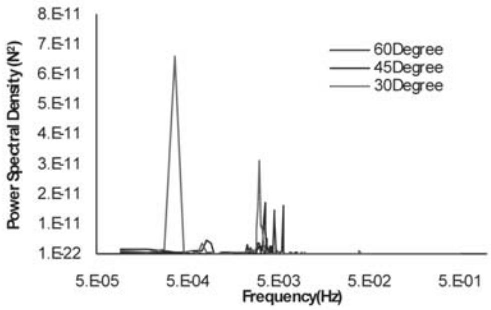

Figure 11. Power spectrum density of static pressure on back arm.

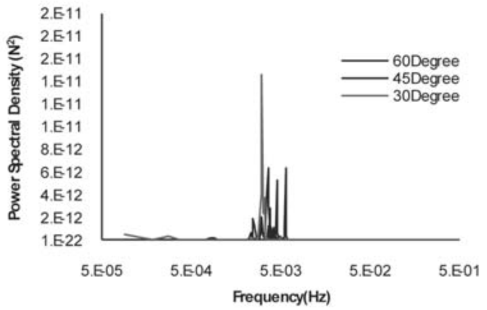

Figure 12. Power spectrum density of static pressure on front arm.

Conclusion

The turbulence flow at downstream of the arm is from the mixing flow between flow across the arm and flow passed the weight saving hole. After comparison of mean static pressure which acting to the arm on each surface and the PSD graph, the 30^o position has most effect from the static pressure. And this could be the source of arm vibration and disc flutter.

Because of the flow passed the weight saving hole induce the vortex flow and the shape of the hole should be the one of factors that may the cause of arm vibration and need to be investigated in the future work.

Acknowledgment

The author would like to express his thank to Mr.Therdthai Thienthong and his team from WD Thailand who supported the data of model and coordinated with the other specialist.

References

Kaneko, S. ,Nishihara, T. and Watanabe, T. 2007. ″Aerodynamic characteristics of carriage arm equipped on hard magnetic disks.″ Springer Microsyst Technol., vol. 13, pp. 1297-1306.

Kubotera, H., Tsuda, N., Tatewaki, M. and Maruyama, T. 2002. ″Aerodynamic vibration mechanism of HDD arms predicted by unsteady numerical simulations.″ IEEE Trans. Mgn., vol. 38, no. 5, pp. 2201-2203, Sep.

Ong, E. H., He, Z., Chen, R., Qian, H. and Guo, G. 2000. ″A low-turbulence-high-bandwidth actuator for 3.5″ hard disk drives,″ IEEE Trans. Mgn., vol. 36, no. 5, pp. 2235-2237, Sep.

Tsuda, N. ,Kubotera, H., Tatewaki, M.,Noda, S., Hashiguchi, M. and Maruyama, T. 2003. ″Unsteady analysis and experimental verification of the aerodynamic vibration mechanism of HDD arms.″ IEEE Trans. Mgn., vol. 39, no. 2, pp. 819-825, Mar.